proceedings

MDPI

Proceedings

Microwave Assisted Synthesis and Its Cytotoxicity Study of 4*H*-Pyrano[2,3-*a*]acridine-3-carbonitrile Intermediate: Experiment Design for Optimization Using Response Surface Methodology †

Selvaraj Mohana Roopan *, Annadurai Bharathi and Duraipandi Devi Priya

Chemistry of Heterocycles & Natural Product Research Laboratory, Department of Chemistry, School of Advanced Science, Vellore Institute of Technology, Vellore 632 014, Tamilnadu, India; bharathiannadurai@gmail.com (A.B.); devipriya.d@vit.ac.in (D.D.P.)

* Correspondence: mohanaroopan.s@vit.ac.in

† Presented at the 23rd International Electronic Conference on Synthetic Organic Chemistry, 15 November–15 December 2019; Available online: https://ecsoc-23.sciforum.net/.

Published: 14 November 2019

Abstract: Several synthetic routes have been achieved to synthesize pyrane fused systems. As a follow up of earlier work, we hereby report the microwave assisted synthesis of key intermediate, pyrane fused acridine compounds **3a–f**. It was obtained by treating α,β-unsaturated ketone **1a–f** and malononitrile **2** in presence of piperidine with ethanolic solution at 50 °C under 200 W power. This method also optimized via microwave method using RSM methodology. All the synthesized derivatives and target compounds were evaluated for cytotoxicity effect on human hepatoblastoma (HepG2) cell line and HDAC enzyme activity.

Keywords: microwave synthesis; RSM; pyrano acridine; cytotoxity

1. Introduction

Pyrane with amine substitution was one of the major classes of heterocycle [1] because their core fragments. It is constituted by a variety of natural products and biologically active compounds [2]. In the latter case, these kinds of compounds have many pharmacological properties and play a major role in biochemical processes [3]. On the other hand, 2-amino-4*H*-pyran-3-carbonitriles act as an important key intermediate for the synthesis of enormous new organic molecules such as pyridine-3-carobnitriles, pyrimidine thiones, pyrano pyrimidines, pyrazolo-3-amines, pyran-3-carbonitrile, chromene-3-carbonitrile, chromenoprimidinone, pyranothiazine, pyranoquinoline, dihydropyridine, dihydropyranopyrrole, dihydrofuro pyridine, pyrimidine dithione, chromenopyrimidine, chromeno pyrimidine thion, triazolopyrimidine respectively [4]. Among many diseases, cancer has been considered to be a genetic disease which occurs as a result of genetic alterations such as deletions, amplifications, point mutations, insertions and translocations [5–7]. The above described genetic reasons are not only the cause for cancer to occur, but it may also involve epigenetic changes which undergoes methylation of DNA and post-translational histone modifications like acetylation, methylation, phosphyralation, etc. [8,9]. With the help of histone post-translational modifications leads to acetylation which provides a link with early gene transcription and chromatin modification. Histone deacetylases (HDAC) and Histone acetyl transferases (HATs) are the two antagonist enzymes, which controls histone acetylation levels. Lysine acetylation was induced by HATs enzymes that is present in core N-terminal histone domains. The removal of acetyl groups from lysine residues is done by Histone deacetylases [10]. Mammalian HDAC family includes eighteen HDAC enzymes and it is further divided into four

groups as follows class I- IV due to their homology sequences of proteins present in the yeast [11]. These classes of HDAC's contain zinc in their catalytic site. Class I HDAC's are predominantly localized within the nucleus [10]. The central role of class I (HDACs) is to control regulation, differentiation and tissue development of cell. These class I HDAC enzymes exert their function by removing histone acetyl groups from tails, which replaced by a non-protein histone complex which regulates the gene expression of cellular process [11]. In class I HDAC, the enzymes 1 and 2 are most probably same this plays a major role from cell growth to apoptosis stage. Cell cycle processes and DNA damage responses are the major roles of HDAC3 enzymes. HDAC8 enzymes are mostly present in cytosol which was expressed by smooth muscle cells for differentiation and plays a major role in tumor cell proliferation.

The RSM (Response Surface Methodology) is an extensively employed mathematical and statistical method for modeling. It is an analysis process where different variables affect the response of interest [12]. The aim of this method is to optimize the response [13]. The parameters influencing the method are called independent variables, while the response is called dependent variables [14]. The RSM explores a suitable relationship of approximation between input and output variables and it also determines the optimum operating conditions for a process under analysis or a factor area region that meets operating requirements [15,16]. Box-Behnken designs (BBD) and central composite design (CCD) are two major experimental designs used in the response surface methodology [13].

Microwave heating has gained attention in the preparation of organic synthesis because of the short treatment time, low energy cost, high heating rate, selective heating, and controllable heating process. Here RSM (Response surface methodology) has been used for microwave optimization to prepare high-performance of pyrane fused acridines **3a–f** to develop various analogues of acridines.

2. Results and Discussion

The current study, the relationship between response (yield of 4*H*-pyrano[2–a]acridine-3-carbonitrile, Table 1) was investigated through RSM. The set of 21 experimental runs via CCD template are showed in Table 2. From the experimental data of Table 2, also, the quadratic model equation the relationship between yield of synthesized compound (response) and the three independent reaction variables were (Table S1) presented (in terms of original factors) by:

$$Y = 89.5843 + 4.61937\ T_i + 1.07703\ W + 5.60598\ T_e - 3.58811\ T_i \times T_i - 5.95508\ W \times W - 10.7015\ T_e \times T_e + 2.42635\ T_i \times W - 1.48761\ T_i \times T_e - 6.01241\ W \times T_e \quad (1)$$

where, Y—Yield of the product; T_i—reaction time; T_e—reaction temperature; W—Wattz used in microwave reactor.

Positive sign before the linear term indicates that the response increases linearly (synergistic influence) with an increase in the parameter, while negative sign indicates antagonistic influence on the other side. For the fitting of quadratic second order model (Table S2), statistical analysis based on variance analysis (ANOVA) was used. Table S2 reflects all the terms of the model for all RSM responses. At a confidence level of 95 percent, the model's F-value of 22.51 and a very low probability value ($p < 0.005$) indicated that the fitted model was very significant.

This also indicated that the regression model used was the accurate one to estimate the final product yield. The model's suitability/fit were evaluated using the regression formula (Equation (1)) and determination coefficient (R^2). A strong determination coefficient value (R^2 0.948) indicated an extraordinary relationship between the independent process variables, which also intended the second order model to be accurate. The model can elucidate at least 94.8% of the data variance. Adequate accuracy ratio of 69.76 was an acceptable signal in the current investigation and showed the model's ability to navigate the development space.

In Figure 1, three-dimensional response surface plots (Figure S1) and two-dimensional contour (interaction) plots are drawn to investigate the individual and interactive effects of system variables on yield. The three-dimensional surfaces are the regression equation's graphical representation. The contour curve (two-dimensional) represented two test variables combined with the other one retained at zero (central value) level. The circular contours have been stated to denote the negligible

interaction between the corresponding variables. Theoretical yield is fitted with the yield obtained (Table 2).

Table 1. Microwave assisted synthesis of compounds **3a–f**.

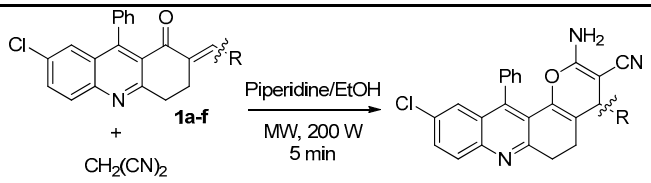

-R	Yield (%)	MP (°C)
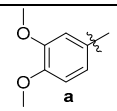 a	90	206–208
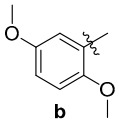 b	82	228–230
 c	84	136–138
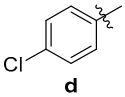 d	82	162–164
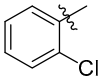 e	82	154–156
 f	83	235–237

Table 2. Experimental analysis of the CCD model **3a–f**.

Time (Min)	Wattz (W)	Temp °C	Theoretical Yield (%)	Experimental Yield (%)
−1	−1	−1	52	52
1	−1	−1	60	62
−1	0	−1	63	63
0	0	−1	73	74
1	0	−1	75	73
−1	1	−1	62	62
0	1	−1	74	72
1	1	−1	79	84
−1	−1	0	76	78
0	−1	0	82	85
1	−1	0	81	78
−1	0	0	81	85
0	0	0	89	90
1	0	0	90	88
−1	1	0	74	73
0	1	0	84	85
1	1	0	88	87
−1	−1	1	79	76
0	−1	1	83	82
1	−1	1	80	84

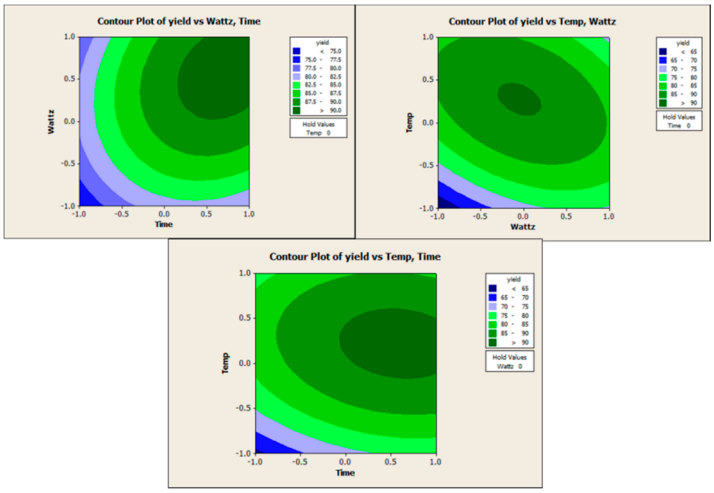

Figure 1. Contour plots for yield optimization using RSM, **3a**.

2.1. Cytotoxicity

All the synthesized compounds (**3a–f**) were subjected to identify its cytotoxicity using MTT assay. Among the various concentrations, 25 mg/mL is elaborated in Figure S2. Data are presented as mean ± SD calculated from the three independent experiments. It shows 29% of mortality after 24 h which results in 41% of cytotoxicity at 100 µg/mL. When it treated with 500 µg/mL the authors inferred the 81.5% of mortality rate were clearly illustrated in (Figure S2).

2.2. Morphological Alterations

To identify the alterations in morphology further the researchers focused on cancer cell line named HepG2 which were treated with several concentrations of synthesized compounds (**3a–f**). With the help of HDAC assay kit morphological alterations were resulted in percentage of HDAC. (Figure S3) Values were expressed as the percentage of HDAC. The Trichostatin A was used as positive control drug. (Figure S4).

2.3. Histone Deacetylase Assay

Inhibition of HDAC activity has been associated with cell-cycle arrest and growth inhibition.

3. Experimental Section

Synthesis of Pyrane Fused Acridines **3a–f**

Synthesis of pyrane fused acridines **3a–f** was achieved by simple conversion from α,β-unsaturated ketone [17,18] and malanonitrile in the presence of ethanol at 50 °C under 200 W powers in a synthesis/extraction reactor of Sineo-UWave-1000 MW-Uv-Us. During this process the reaction has been monitor through thin layer chromatography. We have observed the consumption of all reactant after 5 min (Table 1). Synthesized derivatives were summarized in Table 3. All the synthesized motifs **3a–f** characterization information is denoted in the Table 3.

Table 3. Characterization data.

Compound	Melting Point & GC-MS	FT-IR	^{1}H-NMR & ^{13}C-NMR	Range
2-amino-10-chloro-4-(3,4-dimethoxyphenyl)-12-phenyl-5,6-dihydro-4H-pyrano[2,3-a]acridine-3-carbonitrile (**3a**)	206–208 °C, 521.15/522.1	2372, 2193 (-CN), 3448 (-NH2).	2.07–2.12, 23.57 2.36–2.42, 32.15 2.91–2.98, 42.10, 55.42 3.07–3.14, 55.37 3.7, 111.17 4.0, 111.95 4.9, 118.37 6.75–6.77, 119.65, 119.81, 120.74, 124.45 6.92–6.94, 127.68, 127.88, 128.03, 128.18, 128.55, 128.73, 2 × 129.74, 130.54 7.23–7.24, 130.87, 135.72, 137.47, 139.56, 139.78 7.37, 144.29 7.57–7.58, 148.02, 148.84 7.71–7.74, 158.03 7.97–8.00, 158.98	(m, 1Ha, -CH_2) (m, 1Hb, -CH_2) (m, 1Ha, -CH_2) (m, 1Hb, -CH_2) (s, 6H, 2-OCH_3) (s, 1H, -CH), (s, 2H, -NH_2) (d, *J* = 8 Hz, 2H) (d, *J* = 8 Hz, 1H) (d, *J* = 1.6 Hz, 1H) (m, 2H), (m, 3H), (dd, *J* = 2 Hz, *J* = 2 Hz, 1H) (d, *J* = 8.8 Hz, 1H)
2-amino-10-chloro-4-(2,5-dimethoxyphenyl)-12-phenyl-5,6-dihydro-4H-pyrano[2,3-a]acridine-3-carbonitrile (**3b**)	228–230 °C, 521.1/522.23	3670 (-NH_2), 2835 (-OCH_3), 2198 (-C=N), 1678 (-C=C, Ar).	2.18–2.25, 23.84, 2.39–2.48, 32.95, 2.99–3.07, 35.50, 55.77, 56.56, 59.35 3.10–3.18, 112.34, 112.53, 115.86, 118.35 3.4, 119.68, 120.87, 125.52, 127.60 3.6, 128.07, 128.22, 128.61, 129.07, 3.75, 129.27, 130.25, 130.33, 132.01, 135.31, 138.79, 140.07 3.79, 141.12, 144.93 6.57, 6.72- 151.67, 6.75, 154.15, 6.81–6.83, 158.76, 7.25–7.28, 7.34–7.37 7.51–7.62, 7.91–7.93, 8.15–8.17 158.88	(m, 1Ha, -CH_2), (m, 1Hb, -CH_2), (m, 1Ha, -CH_2), (m, 1Hb, -CH_2), (s, 2H, -NH_2), (s, 1H, -CH), (s, 3H, -OCH_3), (s, 3H, -OCH_3), (s, 1H), (d, *J* = 10 Hz, 1H), (d, *J* = 8.4 Hz, 2H), (d, *J* = 9.6 Hz, 1H), (t, *J* = 14 Hz, 2H), (m, 2H), (d, *J* = 19.6 Hz, 1H), (d, *J* = 9.2 Hz, 1H).

*2-amino-10-chloro-4-(3-methoxyphenyl)-12-phenyl-5,6-dihydro-4H-pyrano[2,3-a]acridine-3-carbonitrile (***3c***)*	136–138 °C, 491.14/492.20	3448 (-NH_2), 2831 (-OCH_3), 2193 (-C=N), 1674 (-C=C, Ar).	2.21–2.28, 24.05, 2.40–2.48, 32.90, 3.01–3.10, 43.25, 55.37, 3.14–3.21, 60.02, 112.77, 114.19 3.49, 117.82, 119.42, 3.81, 120.48, 120.70 4.03, 125.54, 127.66, 128.11 6.79–6.80, 128.27, 128.57, 129.06, 129.24 6.81–6.82, 130.08, 130.29, 130.46, 132.41 6.83–6.84, 138.73, 140.44, 7.29–7.31, 140.96, 144.18, 7.37–7.40, 7.53–7.61, 145.05, 7.94–7.96 158.20, 158.58, 160.19	(m, 1Ha, -CH_2), (m, 1Hb, -CH_2), (m, 1Ha, -CH_2), (m, 1Hb, -CH_2), (s, 2H, -NH_2), (s, 3H, -OCH_3) (s, 1H, -CH), (d, *J* = 1.6 Hz, 1H), (d, *J* = 2 Hz, 1H), (d, *J* = 2.8 Hz, 1H), (m, 2H), (m, 2H), (m, 4H), (d, *J* = 8.8 Hz, 1H).)
*2-amino-10-chloro-4-(4-chlorophenyl)-12-phenyl-5,6-dihydro-4H-pyrano[2,3-a]acridine-3-carbonitrile (***3d***)*	162–164 °C, 495.09/496	2372, 2191 (-CN), 3446 (-NH_2).	2.13–2.20, 24.04, 2.37–2.45, 32.82, 2.99–3.06, 42.75 3.12–3.49, 59.73, 4.0, 117.26, 3.4, 119.22, 120.53, 125.57 7.17, 2 × 127.72, 128.14, 128.32, 128.56, 2 × 129.07 7.19, 129.20, 129.32, 129.42, 130.33 7.26, 130.60 7.30, 132.51 7.32, 133.75, 138.70, 140.64, 141.08 7.35, 141.18, 7.38, 145.13, 7.52–7.60, 158.22, 7.93–7.95. 158.39	(m, 1Ha, -CH_2), (m, 1Hb, -CH_2), (m, 1Ha, -CH_2), (m, 1Hb, -CH_2), (s, 1H, -CH), (s, 2H, -NH_2), (s, 1H), (s, 1H), (s, 1H), (s, 1H), (s, 1H), (d, *J* = 2.4 Hz, 1H), (s, 1H), (m, 4H), (d, *J* = 8.8 Hz, 1H).
*2-amino-10-chloro-4-(2-chlorophenyl)-12-phenyl-5,6-dihydro-4H-pyrano[2,3-a]acridine-3-carbonitrile (***3e***)*	154–156 °C, 495.09/496.46.	3446 (-NH_2), 2191 (-C=N), 1678 (-C=C, Ar).	2.12–2.20, 23.78, 2.40–2.48, 32.79, 2.97–3.05, 58.74, 117.20, 3.12–3.19, 119.17, 120.61, 125.56, 127.71, 127.81 3.52, 128.12 4.76, 128.25 7.12–7.13, 128.54, 2 × 129.10, 129.25 7.18–7.22, 129.40, 130.18, 130.29, 130.52, 130.60, 130.05,	(m, 1Ha, -CH_2), (m, 1Hb, -CH_2), (m, 1Ha, -CH_2), (m, 1Hb, -CH_2), (s, 2H, -NH_2), (s, 1H, -CH), (d, *J* = 3.6 Hz, 1H), (m, 1H), (d, *J* = 6.4 Hz, 1H), (d, *J* = 6.8 Hz, 1H), (d, *J* = 4.8 Hz, 1H),

			7.29–7.30, 7.36–7.37, 132.43, 133.72, 138.65, 140.52 7.46–7.47, 141.23 7.53–7.54, 145.05, 7.50–7.63, 158.55, 7.91–7.94, 8.15–8.18. 158.75	(d, *J* = 5.2 Hz, 1H), (m, 4H), (d, *J* = 3.2 Hz, 1H), (d, *J* = 9.2 Hz, 1H).
2-amino-10-chloro-4,12-diphenyl-5,6-dihydro-4H-pyrano[2,3-a]acridine-3-carbonitrile (**3f**)	235–237 °C, 461.13/462.29	3442 (-NH2), 2204 (-C=N), 1656 (-C=C, Ar)	2.23–2.27, 24.08 3.01–3.09, 32.87 3.14–3.22, 43.27, 60.15 3.50 4.07, 117.94 7.27–7.28, 119.44, 120.71, 124.54, 2 × 127.67, 127.87, 128.07, 128.13, 128.28 7.30–7.31, 128.58, 129.10, 3 × 129.23, 130.29 7.35, 130.47, 132.42, 138.74 7.38–7.40, 140.44, 140.97 7.42, 142.51 7.54–7.58, 145.05 7.59–7.62, 158.18 7.95–7.97, 158.58	(m, 1Ha, -CH_2) (m, 1Ha, -CH_2) (m, 1Hb, -CH_2) (s, 2H, -NH_2) (s, 1H, -CH) (d, *J* = 4.8 Hz, 2H) (m, 2H) (s, 1H) (m, 2H) (s, 1H) (m, 2H) (m, 2H) (d, *J* = 8.8 Hz, 1H)

4. Conclusions

All the synthesized derivatives **3a–f** were subsequently evaluated for cytotoxicity activity by the MTT assay on human hepatocellular carcinoma (HepG2) cell line, after and during a period of about 6 days. The cells were exposed to concentrations of 0% (control), 5%, 10%, 15%, 20% and 25%. The MTT assay resulted in apoptosis of cancer cell line by damaging structure of DNA were observed.

Supplementary Materials: The following are available online at http://www.xxxxx, Figures S1–S4, Tables S1 and S2.

Author Contributions: S.M.R. designed the research plan. S.M.R. and A.B. synthesized the compounds. D.P. performed the RSM. All authors have read and agreed to the published version of the manuscript.

Funding: DST-FTYS (No. SR/FT/CS-264/2012), Government of India, New Delhi.

Acknowledgments Author thank to VIT management for providing research facility and support.

Conflicts of Interest: The authors declare no conflict of interest.

References

1. Al-Omran, F.; Mohareb, R.M.; El-Khair, A.A. Synthesis and *E*/*Z* Configuration Determination of Novel Derivatives of 3-Aryl-2-(benzothiazol-2′-ylthio) Acrylonitrile, 3-(Benzothiazol-2′-ylthio)-4-furan-2″-yl)-3-buten-2-one and 2-(1-(Furan-2″-yl)-3′-oxobut-1''-en-2-ylthio)-3-phenylquinazolin-4(3*H*)-one. *Molecules* **2011**, *16*, 6129–6147.
2. Bhattacharyya, P.; Pradhan, K.; Paul, S.; Das, A.R. Nano crystalline ZnO catalyzed one pot multicomponent reaction for an easy access of fully decorated 4H-pyran scaffolds and its rearrangement to 2-pyridone nucleus in aqueous media. *Tetrahedron Lett.* **2012**, *53*, 4687–4691.
3. Dokmanovic, M.; Clarke, C.; Marks, P.A. Histone deacetylase inhibitors: overview and perspectives. *Mol. Cancer Res*. **2007**, *5*, 981–989.
4. Khan, A.T.; Lal, M.; Ali, S.; Khan, M.M. One-pot three-component reaction for the synthesis of pyran annulated heterocyclic compounds using DMAP as a catalyst. *Tetrahedron Lett*. **2011**, *52*, 5327–5332.
5. Lingaiah, B.P.V.; Reddy, G.V.; Yakaiah, T. Efficient and Convenient Method for the Synthesis of Poly Functionalised 4H-Pyrans. *Synth Commun*. **2004**, *34*, 4431–4437.
6. Pandey, G.; Singh, R.P.; Gary, A.; Singh, V.K. Synthesis of Mannich type products via a three-component coupling reaction. *Tetrahedron Lett.* **2005**, *46*, 2137–2140.
7. Roopan, S.M.; Bharathi, A.; Palaniraja, J.; Anand, K.; Gengan, R.M. Unexpected regiospecific Michael addition product: synthesis of 5,6-dihydrobenzo[1,7]phenanthrolines. *RSC Adv*. **2015**, *5*, 38640–38645.
8. Williams, D.R.; Heidebrecht, R.W. Total Synthesis of (+)-4,5-Deoxyneodolabelline. *J. Am. Chem. Soc*. **2013**, *125*, 1843–1850.
9. Xu, W.; Huang, H.C.; Lin, C.J.; Jiang, Z.F. Chitooligosaccharides protect rat cortical neurons against copper induced damage by attenuating intracellular level of reactive oxygen species. *Bioorg. Med. Chem. Lett*. **2010**, *20*, 3084–3088.
10. Yang, Y.; Haung, Y.; Qing, F.L. Asymmetric synthesis of trifluoromethylated aziridines from CF3-substituted N-tert-butanesulfinyl ketimines. *Tetrahedron Lett*. **2013**, *29*, 3826–3830.
11. Zahonero, B.B.; Parra, M. Histone deacetylases and cancer. *Mol. Oncol*. **2012**, *6*, 579–589.
12. Refinery, N.P.; Braimah, M.N. Utilization of Response Surface Methodology (RSM) in the Optimization of Crude Oil Refinery Process, New Port-Harcourt Refinery, Nigeria. *J. Multidis. Eng. Sci. Tech. (JMEST)* **2016**, *3*, 4361–4369.
13. Montgomery, D.C. *Introduction to Statistical Quality Control*; John Wiley and Sons, Inc.: Hoboken, NJ, USA, 2005.
14. Koç, B.; Kaymak-Ertekin, F. Research surface methodology and food processing applications. *Gıda* **2009**, 7, 1–8.
15. Bradley, N. The Response Surface Methodology. Master's Thesis, Indiana University South Bend, South Bend, IN, USA, 2007.

16. Farooq, Z.; Rehman, S.; Abid, M. Application of response surface methodology to optimize composite flour for the production and enhanced storability of leavened flat bread (Naan). *J. Food Process Pres.* **2013**, *37*, 939–945.
17. Pishgar-Komleh, S.H.; Keyhani, A.; Msm, R.; Jafari, A. Application of Response Surface Methodology for Optimization of Picker-Husker Harvesting Losses in Corn Seed. *Iran. J. Energy Environ*. **2012**, *3*, 134–142.
18. Roopan, S.M.; Bharathi, A.; Al-Dhabi, N.A.; Arasu, M.V.; Madhumitha, G. Synthesis and insecticidal activity of acridone derivatives to Aedes aegypti and Culex quinquefasciatus larvae and non-target aquatic species. *Sci. Rep*. **2017**, *7*, 39753.

© 2019 by the authors. Licensee MDPI, Basel, Switzerland. This article is an open access article distributed under the terms and conditions of the Creative Commons Attribution (CC BY) license (http://creativecommons.org/licenses/by/4.0/).